

## Research Article

# Transverse Momentum and Pseudorapidity Dependence of Particle Production in Xe–Xe Collision at $\sqrt{s_{NN}} = 5.44$ TeV

Zhang-Li Guo <sup>1,2</sup>, Bao-Chun Li <sup>1,2</sup> and Hong-Wei Dong <sup>1,2</sup>

<sup>1</sup>College of Physics and Electronics Engineering, State Key Laboratory of Quantum Optics and Quantum Optics Devices, Shanxi University, Taiyuan 030006, China

<sup>2</sup>Collaborative Innovation Center of Extreme Optics, Shanxi University, Taiyuan 030006, China

Correspondence should be addressed to Bao-Chun Li; libc2010@163.com

Received 9 June 2019; Revised 6 September 2019; Accepted 1 October 2019; Published 1 February 2020

Guest Editor: Sakina Fakhraddin

Copyright © 2020 Zhang-Li Guo et al. This is an open access article distributed under the Creative Commons Attribution License, which permits unrestricted use, distribution, and reproduction in any medium, provided the original work is properly cited. The publication of this article was funded by SCOAP<sup>3</sup>.

Through the collision-system configuration, the Tsallis statistics is combined with a multisource thermal model. The improved model is used to investigate the transverse momentum and pseudorapidity of particles produced in Xe–Xe collisions at  $\sqrt{s_{NN}} = 5.44$  TeV. We discuss detailedly the thermodynamic properties, which are taken from the transverse momentum  $p_T$  distributions of  $\pi$ ,  $K$ , and  $p$  for different centralities. The pseudorapidity  $\eta$  spectra of charged particles for different centralities are described consistently in the model. And, the model result can estimate intuitively the longitudinal configuration of the collision system.

## 1. Introduction

The important goal of the ultrarelativistic heavy-ion collisions is to find and study the Quark–Gluon Plasma (QGP), which is a new matter state of strongly interacting quarks and gluons at high temperature and density [1–3]. From 2010 to 2019, the Large Hadron Collider (LHC) has mainly carried out  $p$ - $p$ ,  $p$ -Pb, and Pb–Pb collision experiments at various collision energies, which can provide different types of collision-system configurations. In 2017, the LHC performed a different kind of hadron collision at high energy, i.e. the first Xe<sup>129</sup> ion collisions at  $\sqrt{s_{NN}} = 5.44$  TeV [4–7]. Since the nucleons of the Xe<sup>129</sup> nucleus is fewer than that of Pb<sup>208</sup> nucleus, the investigation of Xe-ion collisions can roughly bridge or connect the gap between  $p$  and Pb ion collisions. As a good intermediate-size system, the Xe–Xe colliding system brings a wonderful opportunity to discuss the colliding-system size dependence of multiparticle production in high-energy nuclear collisions [8, 9]. The nucleus collisions at high energies offer numerous experimental data about charged particle production, such as pions, kaons, and protons. The particle production in the collision contains the interaction effects between hard and soft QCD processes. The feature discussion of the particle distribution can be used to infer the evolution and dynamics of different collision systems at different center of mass energies.

With respect to the final-state observables in these collisions, the particle transverse momentum and pseudorapidity

multiplicity are two key measurements to understand the particle-production process and the matter evolution under the extreme conditions. The transverse momentum spectra are very important because they can provide essential information about QGP created in the collisions. The charged-particle pseudorapidity multiplicity is related to the early geometry of the collision system and is of great interest to investigate the properties of the collision-system evolution. Recently, the ALICE Collaboration measured charged-particle transverse momentum spectra and multiplicity density in Xe–Xe collisions at  $\sqrt{s_{NN}} = 5.44$  TeV at the LHC [5, 6]. In this work, the transverse momentum spectra are analyzed in an improved multisource thermal model, where the Tsallis statistics [10–13] is imported. Combined with the collision picture, we also discuss the charged-particle pseudorapidity density for different collision centralities. The investigation of the particle production in different collision systems can help us understand the matter evolution in the different collisions.

## 2. The Particle Spectra in the Improved Multisource Thermal Model

In high-energy nucleon or nuclei collisions, the thermodynamic information of the system evolution is very rich. These identified particles produced in the collisions may be regarded as a multiparticle system. The identified particles emit from

different sources. We can assume that many emission sources are formed in the interacting system [14–17]. In the stationary reference frame of a considered source, the distribution function of the particle momentum  $p'$  is given by

$$f_{p'}(p') = \frac{1}{N} \frac{dN}{dp'} = Cp'^2 \left[ 1 + (q-1) \frac{\sqrt{p'^2 + m_0^2} - \mu}{T} \right]^{-q/(q-1)}, \quad (1)$$

where  $C$ ,  $T$ , and  $q$  is the normalization constant, the temperature and the nonequilibrium degree parameter, respectively. The  $q$  value is close to 1. For the chemical potential  $\mu = 0$ , the distribution function is

$$f_{p'}(p') = \frac{1}{N} \frac{dN}{dp'} = Cp'^2 \left[ 1 + (q-1) \frac{m_T}{T} \right]^{-q/(q-1)}. \quad (2)$$

When  $q$  tends to 1, the density function is the standard Boltzmann distribution. The particle momentum function  $p' = g(R_1)$  can be obtained by the Monte Carlo calculation,  $\int_0^{p'} f(p') dp' < R_1 < \int_0^{p'+dp'} f(p') dp'$ . The particle rapidity  $y'$  is

$$y' = \frac{1}{2} \ln \frac{E' + p'_z}{E' - p'_z}, \quad (3)$$

where  $E'$  and  $p'_z = p' \cos \theta'$  is the energy and longitudinal momentum, respectively. The pseudorapidity and the transverse momentum are

$$\eta' = -\ln \left[ \tan \frac{\theta'}{2} \right] = \frac{1}{2} \ln \left( \frac{p' + p'_z}{p' - p'_z} \right), \quad (4)$$

$$p'_T = \sqrt{p'^2_x + p'^2_y} = p' \sin \theta', \quad (5)$$

where  $\theta' = \arctan [2 \sqrt{r_2(1-r_2)} / (1-2r_2)]$  is the particle emission angle and is calculated by the Monte Carlo method. The parameter  $r_2$  is a random number distributed evenly in  $[0, 1]$ . Due to  $p_T = p'_T$ , the distribution function of the particle transverse-momentum in the laboratory reference system frame is

$$f_{p_T}(p_T) = \frac{1}{N} \frac{d^2N}{dp_T d\eta} = C_T p_T m_T \cosh \eta' \left[ 1 + (q-1) \frac{m_T \cosh \eta'}{T} \right]^{-q/(q-1)}. \quad (6)$$

In contrast to the transverse momentum, the particle pseudorapidity  $\eta$  in the laboratory reference system frame is not easy to calculate. Since  $\eta'$  is a result of the source reference frame, one source is only considered in Equation (1). For the calculation of the pseudorapidity, the space scale of the collision system cannot be ignored at the pseudorapidity  $\eta$  space. Along the beam, these sources can be grouped into four categories as follows: a projectile leading-particle source with a pseudorapidity shift  $\eta_{plp}$ , a projectile cylinder composed of a series of sources with pseudorapidity shifts  $\eta_{pc}$  ( $\eta_{pc}^{\min} \leq \eta_{pc} \leq \eta_{pc}^{\max}$ ), a target cylinder composed of a series of sources with pseudorapidity shifts  $\eta_{tc}^{\min} \leq \eta_{tc} \leq \eta_{tc}^{\max}$  and a target leading-particle

source with a pseudorapidity shift  $\eta_{tlp}$ . In the laboratory reference system frame, the Monte Carlo pseudorapidity function of particles from the four parts can be written as

$$\eta_1 = \eta_{plp} + \eta', \quad (7)$$

$$\eta_2 = \eta_{pc} + \eta', \quad \eta_{pc}^{\min} \leq \eta_{pc} \leq \eta_{pc}^{\max}, \quad (8)$$

$$\eta_3 = \eta_{tc} + \eta', \quad \eta_{tc}^{\min} \leq \eta_{tc} \leq \eta_{tc}^{\max}, \quad (9)$$

$$\eta_4 = \eta_{tlp} + \eta'. \quad (10)$$

By the  $p'$  distribution function Equation (1), we can obtain the source pseudorapidity  $\eta'$  in the stationary reference frame. Then, the pseudorapidity distribution in the laboratory reference frame can be derived from the  $\eta$  space scale of the collision system, which is described by the collision Equations (9) and (10).

### 3. Discussions and Conclusions

Figure 1 shows transverse momentum  $p_T$  distributions of pions  $\pi$ , kaons  $K$  and protons  $p$  produced in Xe–Xe collisions at  $\sqrt{s_{NN}} = 5.44$  TeV. The filled circles indicate the experimental data [5] for nine centrality bins (from 0% to 5% central collisions to 70–80% peripheral collisions). The lines are the results of the Equation (6). For pions, kaons and protons, the nonequilibrium degrees are  $q = 1.141$ ,  $q = 1.080$  and  $q = 1.022$ , respectively. For the same particles, the  $q$  is a constant value in each interval of the centrality. This reflects nonequivalent excitation of the thermal sources of the three particles in the centrality classes. The temperatures for the three kinds of particles are shown in Tables 1–3 with  $\chi^2/\text{ndf}$  and increase with the increase of the collision centrality. The  $p_T$  differential cross sections for different collision centralities are governed by the temperature  $T$ , where the reaction system freezes out and the considered particles will no longer interact. The particles at low  $p_T$  region are more close to a thermal equilibrium and the particles at high  $p_T$  region are more close to be produced in a hard scatterings, which is determined by pQCD [18, 19]. The temperature is used to reflect quantitatively the excitation of emission sources of final-state particles.

From pions to protons, these particle masses affect the slope of the transverse momentum  $p_T$  spectra. So, the temperature  $T$  and nonequilibrium degree  $q$  depend on the final-state particle mass. With increasing particle mass, the temperature  $T$  increases generally and the nonequilibrium degree  $q$  decreases. The mass dependence may originate from the deformed nuclei, Xe. With the matter produced in the collision moving at a finite velocity, the Lorentz-boost magnitude of the momentum distribution occurs obviously and is proportional to the particle mass. Therefore, the  $q$  values of  $\pi$ ,  $K$  and  $p$  systems are different. This shows how close the three systems are to the kinetic equilibrium.

Figure 2 shows pseudorapidity  $\eta$  spectra of charged particles produced in Xe–Xe collisions at  $\sqrt{s_{NN}} = 5.44$  TeV. The filled circles indicate the experimental data [6] for twelve centrality bins (from 0% to 2.5% central collisions to 80–90% peripheral collisions). The lines are the results of the Equations

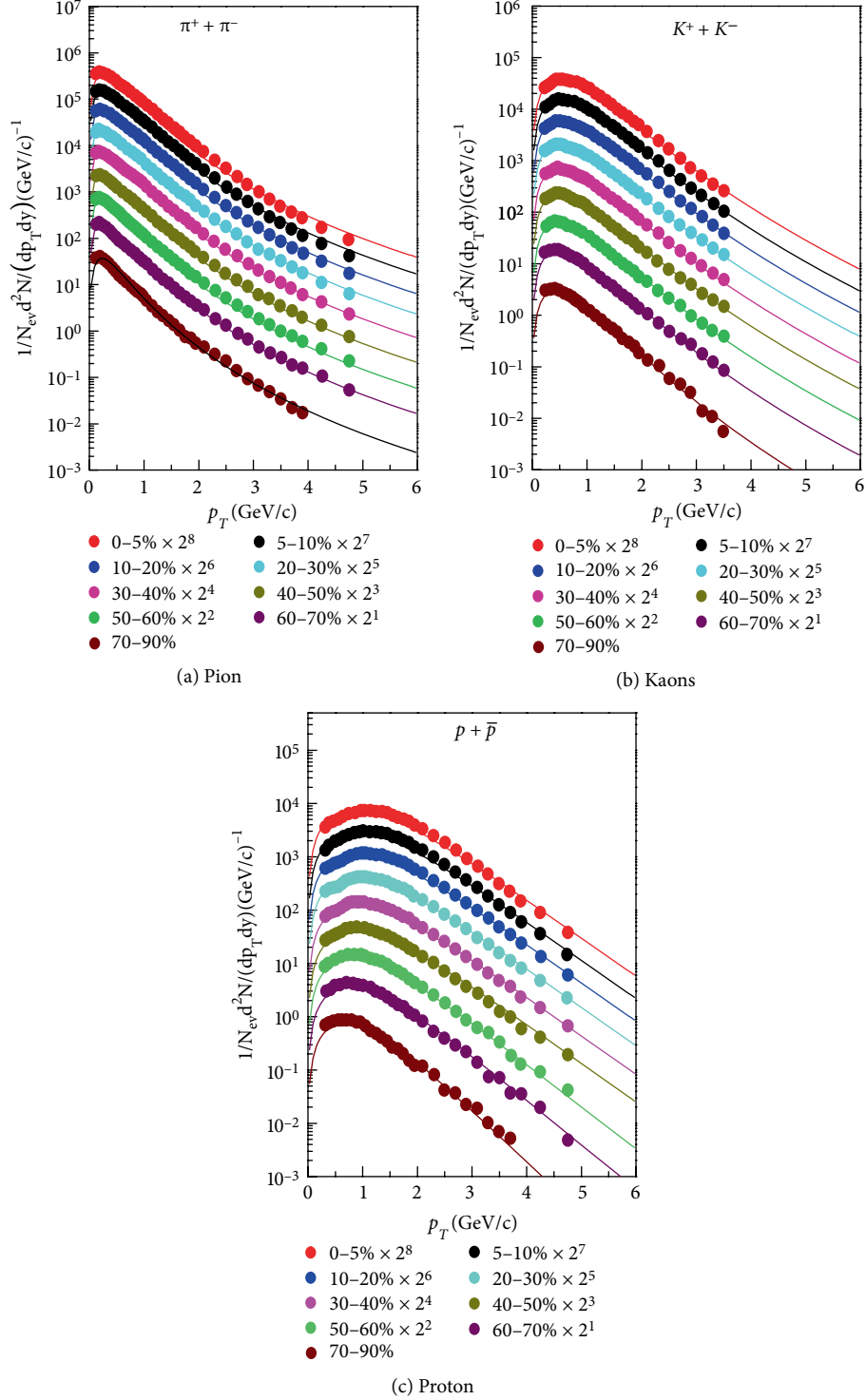


FIGURE 1: Transverse momentum distributions of  $\pi$ ,  $K$  and  $p$  in Xe-Xe collisions at  $\sqrt{s_{NN}} = 5.44$  TeV. The filled circles indicate the experimental data in nine centrality bins [5]. The lines are the results of Equation (6).

(7)–(10). The heights of the pseudorapidity spectra exhibit strong centrality dependences. It is because the number of observed particles is approximately proportional to the number of collision participant nucleons, which is a function of the impact parameter [20–23]. The configuration parameters of the thermalized cylinder are shown in Table 4. The  $\eta_{pc}^{\max}$  and

$\eta_{pc}^{\min}$  slightly increase with collision centralities. The pseudorapidity distributions of the peripheral collision are wider than that of the most central collision. So, the length of the thermalized cylinder at  $\eta$  space decreases with the impact parameter. It means the number of thermal sources produced in Xe-Xe collision increases with centralities. The source

TABLE 1: Values of parameters used in Figure 1(a). The unit of  $T$  is GeV.

Centrality	$T$	$\chi^2/\text{ndf}$
0–5%	0.101	0.447
5–10%	0.100	0.283
10–20%	0.099	0.124
20–30%	0.098	0.150
30–40%	0.097	0.202
40–50%	0.096	0.261
50–60%	0.095	0.312
60–70%	0.094	0.286
70–90%	0.091	0.472

TABLE 2: Values of parameters used in Figure 1(b). The unit of  $T$  is GeV.

Centrality	$T$	$\chi^2/\text{ndf}$
0–5%	0.202	0.165
5–10%	0.200	0.160
10–20%	0.199	0.144
20–30%	0.198	0.105
30–40%	0.196	0.275
40–50%	0.195	0.369
50–60%	0.191	0.424
60–70%	0.183	0.571
70–90%	0.166	0.601

TABLE 3: Values of parameters used in Figure 1(c). The unit of  $T$  is GeV.

Centrality	$T$	$\chi^2/\text{ndf}$
0–5%	0.382	0.317
5–10%	0.381	0.295
10–20%	0.379	0.210
20–30%	0.378	0.226
30–40%	0.377	0.305
40–50%	0.374	0.514
50–60%	0.342	0.590
60–70%	0.324	0.646
70–90%	0.278	0.675

contributions from different categories are seen intuitively and the configuration of the collision system is quantized visually. It helps us understand the influence of the collision-system size and the evolution information of the produced matter in the collision [24, 25].

In reference [6], the experimental data of the pseudorapidity spectra in Xe–Xe collision at  $\sqrt{s_{NN}} = 5.44\text{TeV}$  are first presented. In this paper, the Tsallis statistics is combined with the collision-system configuration, i.e., the multisource thermal model. The improved model is used to investigate the particle production in the intermediate-size collision system, Xe–Xe collision [20, 26]. By the study of the transverse momentum  $p_T$  distributions of  $\pi$ ,  $K$  and  $p$ , the temperature and nonequilibrium degree are obtained. The centrality dependence and the particle mass

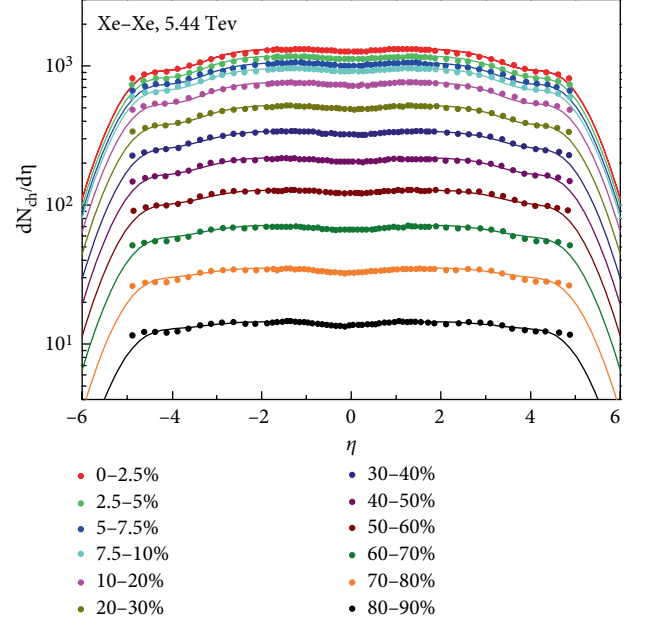


FIGURE 2: Pseudorapidity density of charged particles produced in Xe–Xe collisions at  $\sqrt{s_{NN}} = 5.44\text{TeV}$ . The filled circles indicate the experimental data in 12 centrality bins [6]. The lines are the results of the Equations (7)–(10).

TABLE 4: Values of parameters corresponding to the curves in Figure 2.

Centrality	$\eta_{pc}^{\max}$	$\eta_{pc}^{\min}$	$\eta_{plp}$	$k$
0–2.5%	3.70	0.05	4.60	0.101
2.5–5%	3.70	0.05	4.60	0.101
5–7.5%	3.70	0.07	4.60	0.101
10–20%	3.70	0.06	4.60	0.101
20–30%	3.75	0.06	4.60	0.101
30–40%	3.80	0.06	4.60	0.101
40–50%	3.80	0.06	4.60	0.101
50–60%	3.85	0.06	4.60	0.101
60–70%	3.90	0.06	4.60	0.101
70–80%	3.95	0.06	4.60	0.101
80–90%	4.00	0.06	4.60	0.101

dependence are discussed. Based on the result, the pseudorapidity  $\eta$  spectra of charged particles are reproduced. The model can describe both transverse momentum spectra and pseudorapidity spectra. The configuration of the intermediate-size collision system is quantized visually by the collision picture, which can characterize the primary properties of the collision system.

## Data Availability

Our paper is a theoretical investigation. This paper has explained how to calculate the theoretical results in detail.

## Conflicts of Interest

The authors declare that they have no conflicts of interest.

## Acknowledgments

This work is supported by National Natural Science Foundation of China under Grants No. 11247250 and No. 11575103, Shanxi Provincial Natural Science Foundation under Grant No. 201701D121005, and Scientific and Technological Innovation Programs of Higher Education Institutions in Shanxi (STIP) Grant No. 201802017.

## References

- [1] B. I. Abelev, M. M. Aggarwal, Z. Ahammed et al., “Azimuthal charged-particle correlations and possible local strong parity violation,” *Physical Review Letters*, vol. 103, p. 251601, 2009.
- [2] J. Adam, D. Adamová, M. M. Aggarwal et al., “Correlated event-by-event fluctuations of flow harmonics in Pb-Pb collisions at  $\sqrt{s_{NN}} = 2.76$  TeV,” *Physical Review Letters*, vol. 117, no. 22, p. 182301, 2016.
- [3] K. Tuchin, “Particle production in strong electromagnetic fields in relativistic heavy-ion collisions,” *Advances in High Energy Physics*, vol. 2013, Article ID 490495, 34 pages, 2013.
- [4] S. Acharya, F. T. Acosta, D. Adamová et al., “Inclusive  $J/\psi$  production in Xe-Xe collisions at  $\sqrt{s_{NN}} = 5.44$  TeV,” *Physics Letters B*, vol. 785, pp. 419–428, 2018.
- [5] S. Ragoni, “Production of pions, kaons and protons in Xe-Xe collisions at  $\sqrt{s_{NN}} = 2.76$  TeV,” *Proceedings of Science Large Hadron Collider Physics*, vol. 2018, p. 085, 2018.
- [6] S. Acharya, F. Torres-Acosta, D. Adamová et al., “Centrality and pseudorapidity dependence of the charged-particle multiplicity density in Xe-Xe collisions at  $\sqrt{s_{NN}} = 5.44$  TeV,” *Physics Letters B*, vol. 790, pp. 35–48, 2019.
- [7] D. S. D. Albuquerque [ALICE Collaboration], “Hadronic resonances, strange and multi-strange particle production in Xe-Xe and Pb-Pb collisions with ALICE at the LHC,” *Nuclear Physics A*, vol. 982, pp. 823–826, 2019.
- [8] B. Kim [ALICE Collaboration], “ALICE results on system-size dependence of charged-particle multiplicity density in p-Pb, Pb-Pb and Xe-Xe collisions,” *Nuclear Physics A*, vol. 982, p. 279, 2019.
- [9] F. Bellini [ALICE Collaboration], “Testing the system size dependence of hydrodynamical expansion and thermal particle production with  $\pi$ , K, p, and  $\phi$  in Xe-Xe and Pb-Pb collisions with ALICE,” *Nuclear Physics A*, vol. 982, pp. 427–430, 2019.
- [10] C. Tsallis, “Possible generalization of Boltzmann-Gibbs statistics,” *Journal of Statistical Physics*, vol. 52, no. 1–2, pp. 479–487, 1988.
- [11] B. I. Abelev, J. Adams, M. M. Aggarwal et al., “Strange particle production in  $p+p$  collisions at  $\sqrt{s} = 200$  GeV,” *Physical Review C*, vol. 75, no. 6, p. 064901, 2007.
- [12] J. Cleymans and D. Worku, “The Tsallis distribution in proton-proton collisions at  $\sqrt{s_{NN}} = 0.9$  TeV at the LHC,” *Journal of Physics G: Nuclear and Particle Physics*, vol. 39, no. 2, p. 025006, 2012.
- [13] Z. Tang, Y. Xu, L. Ruan, G. van Buren, F. Wang, and Z. Xu, “Spectra and radial flow in relativistic heavy ion collisions with Tsallis statistics in a blast-wave description,” *Physical Review C*, vol. 79, no. 5, p. 051901, 2009.
- [14] B. C. Li, Y. Y. Fu, L. L. Wang, E. Q. Wang, and F. H. Liu, “Transverse momentum distributions of strange hadrons produced in nucleus-nucleus collisions at  $\sqrt{s_{NN}} = 5.44$  and 200 GeV,” *Journal of Physics G: Nuclear and Particle Physics*, vol. 39, no. 2, p. 025009, 2012.
- [15] B. C. Li, Y. Y. Fu, L. L. Wang, and F. H. Liu, “Dependence of elliptic flows on transverse momentum and number of participants in Au+Au collisions at  $\sqrt{s_{NN}} = 200$  GeV,” *Journal of Physics G: Nuclear and Particle Physics*, vol. 40, no. 2, p. 025104, 2013.
- [16] S. K. Tiwari and C. P. Singh, “Particle production in ultrarelativistic heavy-ion collisions: a statistical-thermal model review,” *Advances in High Energy Physics*, vol. 2013, Article ID 805413, 27 pages, 2013.
- [17] J. Yang, Y. Y. Ren, and W. N. Zhang, “Pion transverse momentum spectrum, elliptic flow, and interferometry in the granular source model for RHIC and LHC heavy ion collisions,” *Advances in High Energy Physics*, vol. 2015, Article ID 846154, 18 pages, 2015.
- [18] J. Adam, D. Adamová, M. M. Aggarwal et al., “Multiplicity dependence of charged pion, kaon, and (anti)proton production at large transverse momentum in p-Pb collisions at  $\sqrt{s_{NN}} = 5.02$  TeV,” *Physics Letters B*, vol. 760, p. 720, 2016.
- [19] G. Giacalone, J. Noronha-Hostler, M. Luzum, and J. Y. Ollitrault, “Confronting hydrodynamic predictions with Xe-Xe data,” *Nuclear Physics A*, vol. 982, pp. 371–374, 2019.
- [20] B. G. Zakharov, “Monte Carlo Glauber model with meson cloud: predictions for 5.44 TeV Xe + Xe collisions,” *The European Physical Journal C*, vol. 78, no. 5, p. 427, 2018.
- [21] M. L. Miller, K. Reygers, S. J. Sanders, and P. Steinberg, “Glauber modeling in high-energy nuclear collisions,” *Annual Review of Nuclear and Particle Science*, vol. 57, no. 1, pp. 205–243, 2007.
- [22] M. Alvioli, H. Holopainen, K. J. Eskola, and M. Strikman, “Initial-state anisotropies and their uncertainties in ultrarelativistic heavy-ion collisions from the Monte Carlo Glauber model,” *Physical Review C*, vol. 85, no. 3, p. 034902, 2012.
- [23] M. Biyajima and T. Mizoguchi, “Analyses of multiplicity distributions and Bose-Einstein correlations at the LHC using negative binomial distribution and generalized Glauber-Lachs formula,” *The European Physical Journal A*, vol. 54, no. 6, p. 105, 2018.
- [24] S. Acharya, F. Torres-Acosta, D. Adamová et al., “Inclusive  $J/\psi$  production in Xe-Xe collisions at  $\sqrt{s_{NN}} = 5.44$  TeV,” *Physics Letters B*, vol. 785, pp. 419–428, 2018.
- [25] S. Tripathy, S. De, M. Younus, and R. Sahoo, “Predictions for azimuthal anisotropy in Xe+Xe collisions at  $\sqrt{s_{NN}} = 5.44$  TeV using a multiphase transport model,” *Physical Review C*, vol. 98, p. 064904, 2018.
- [26] K. J. Eskola, H. Niemi, R. Paatelainen, and K. Tuominen, “Predictions for multiplicities and flow harmonics in 5.44 TeV Xe+Xe collisions at the CERN Large Hadron Collider,” *Physical Review C*, vol. 97, no. 3, p. 034911, 2018.